AIAA 80-0127R

Computational and Simplified Analytical Treatment of Transonic Wing/Fuselage/Pylon/Store Interactions

Vijaya Shankar* and Norman Malmuth†
Rockwell International, Thousand Oaks, Calif.

Transonic modified small-disturbance theory has been employed to numerically model the flowfield around wing/fuselage/pylon/store configurations. A fine grid region enclosing the wing/pylon/store is embedded within a global crude grid and a successive crude-fine relaxation is performed. Using an image point concept, the store and the pylon are introduced into an existing wing/fuselage program, thus avoiding excessive additional computer memory requirements. Comparison of results with experiments on the F-5 wing with a pylon/store arrangement is presented showing good agreement. A study of the roles of pylon height, store diameter, pylon span mount location, angle of attack, and Mach number relative to the achievement of optimum L/D from beneficial nonlinear interference is presented. In addition, a simplified analytical approach to compute the loading on the store using an "immersion theory" is indicated and validated against experiments.

Introduction

ALTHOUGH the problem of external store interference has been of interest for many years, cost effective and systematic methods for predicting separation and achieving optimum aerodynamic integration are in their infancy. Because of the myriad of parameters associated with typical installations, design solutions have been obtained principally through the use of wind-tunnel testing. This approach has several drawbacks, including the realization of suboptimal solutions, the increasing costs of adequate simulations, and the difficulty of experimentally modeling free-field flight conditions—with particular emphasis on sting and wall interference effects. These experimental problems are aggravated in the transonic regime with additional uncertainties regarding the upstream Mach number environment.

The problem has taken on increased significance recently in the wake of the emphasis on energy-efficient aircraft such as span loaders and the increasing use of air-launched missiles such as the ASALMs. From an integration viewpoint, recent studies have indicated the possibility of minimizing or even reversing L/D penalties associated with fuel pod or weapons carriage. These gains are associated, at least in part, with the interruption of spanwise flow and an effective end-plate effect of the store arrangement. Furthermore, streamwise positioning can create exciting possibilities for wave drag reduction through altered area ruling. Relatively small percentage gains in L/D from winglets such as those utilized on the DC-10 and KC-135 have been reported to translate into enormous savings (on the order of 10^5 gal of oil annually when applied over a military air transport fleet). With respect to store separation, suck-back of the weapon on supersonic release has been a dangerous problem that is receiving attention currently at NASA. Similar catastrophic conditions can occur transonically and require corresponding attention to avoid loss of the aircraft and provide safe launch envelopes. Current practice in defining weapon separation characteristics is to utilize questionable pseudosteady-based wind-tunnel grid techniques to provide inputs to trajectory codes. To reduce the cost of this approach (which may be prohibitive), some type of predictive technique is required for the nonlinear transonic regime.

For these needs, methods based on linearized models such as the Prandtl-Glauert theory have been used to treat the associated nonplanar flows. Codes based on vortex lattice and panel methods are being used extensively to handle complex geometries and are an attractive supplement to the wind tunnel, providing that the assumptions of linear theory can be met. Nonlinearities, mixed flow conditions, and shock waves in the transonic regime degrade the validity of results obtained with the Prandtl-Glauert theory and the area rule. The success of small-disturbance and full-potential equation models in handling simpler three-dimensional configurations such as isolated wings and wing/body combinations leads to the expectation that they can be applied successfully to treat the store interference problem.

The scope of this paper is twofold: 1) the development of a complete numerical procedure to treat a wing/fuselage/pylon/store configuration based on the modified small-disturbance (MSD) theory is discussed; and 2) the application of simplified analytical/computational approaches that can be of value in store separation calculations from an engineering design viewpoint is indicated. One of the simplified approaches to be reported in this paper involves an "immersion concept" in which the store/pylon configuration is thought of as being immersed in an effective downwash field created by the parent wing/fuselage configuration. The normal loads on the store are then predicted based on slender body theory and an incidence field which is obtained from the MSD computational flow solution for an isolated wing or wing/fuselage combination.

Although the basic wing/fuselage/pylon/store configuration to be considered in this paper is simple (single pylon with a single axisymmetric store) compared to more realistic arrangements (multiple pylons with multiple store racks), it is sufficiently complex to make small-disturbance theory preferable to a formulation based on the full potential equation from a computational modeling standpoint. Accordingly, the MSD theory code originally developed by Ballhaus et al.[1] and later refined by Mason et al.[2] to treat wing/fuselage configurations has been used in our algorithm as a basic framework into which the pylon and the store components are added. In spite of the significant discrepancies between the measured and predicted lower surface pressure values for certain configurations reported in Ref. 2, their MSD code was chosen for its geometric flexibility and wide industry usage. In particular, the pylon and the store treatment to be reported in this paper is not code dependent

Presented as Paper 80-0127 at the AIAA 18th Aerospace Sciences Meeting, Pasadena, Calif., Jan. 14-16, 1980; submitted Jan. 28, 1980; revision received Sept. 26, 1980.

*Member Technical Staff, Science Center. Member AIAA.
†Project Manager, Fluid Mechanics, Science Center. Associate Fellow AIAA.

and is easily transferable to future more refined wing/fuselage codes which deal effectively with these difficulties.

Excessive additional computer memory requirements and execution time have been avoided by using a simple image point concept for imposing the store and pylon boundary conditions. This approach resembles that employed for the wing treatment in the inverse code of Ref. 3. Herein, the logic for the pylon is such that it can accommodate the tip-mounted winglet system as a special case. In the computational procedure, a fine grid region enclosing the wing/pylon/store is embedded within a global crude grid arrangement and a successive crude-fine relaxation is performed.

Comparison of computational results from this model against experiments[4] for F-5 wing/pylon/store combinations is presented in the Results section. In addition, parametric studies of the effects of pylon height, span location, and store diameter on a basic wing/fuselage configuration used by Alford et al.[5] are also reported. These results clearly indicate the possibility for achieving optimum aerodynamic integration of a pylon/store relative to the parent configuration by proper orientation. A simplified immersion concept is also described which can provide loads on the store for pseudosteady store separation trajectory modeling at a small additional expense over that associated with parent configuration computational solutions. Such information is vital to the understanding of factors associated with safe launch and jettison and avoidance of collision of the store with the aircraft.

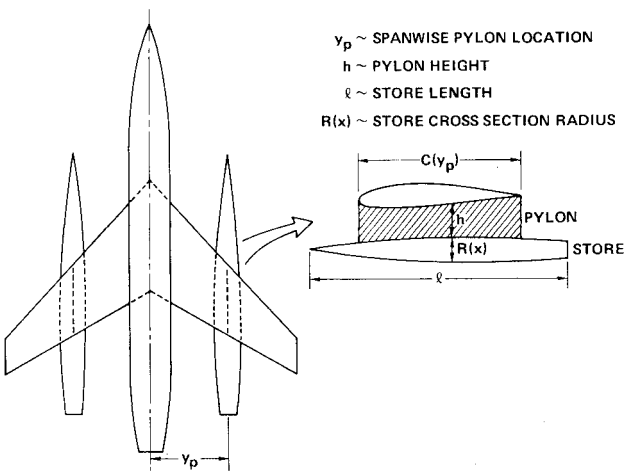

Fig. 1 Simple wing/fuselage/pylon/store configuration.

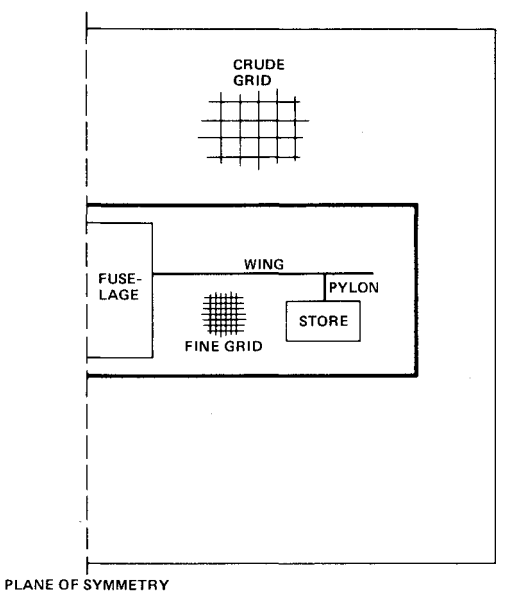

Fig. 2 Crude grid/fine grid arrangement in the computational plane.

Computational Approach

A typical wing/fuselage/pylon/store configuration is schematically indicated in Fig. 1. To analyze the flowfield of this geometry at transonic speeds, the following modified small-disturbance theory equation in conservation form is used

$$\left[(1-M_\infty^2)\phi_x-\left(\frac{\gamma+1}{2}\right)M_\infty^{1.75}\phi_x^2+\left(\frac{\gamma-3}{2}\right)M_\infty^2\phi_y^2\right]_x + [\phi_y-(\gamma-1)M_\infty^2\phi_x\phi_y]_y+(\phi_z)_z=0 \quad (1)$$

Equation (1) does not contain cross-derivative terms such as ϕ_{zx} which may be important in the vicinity of the store/pylon. These will be considered in future investigations. One of the objectives of the present study is to establish the feasibility of an image point concept to incorporate the store/pylon with little programming effort and additional storage requirement.

The handling of the boundary condition for the wing and fuselage has already been reported in Refs. 2 and 3 and will not be discussed in this paper. Only the pylon and store treatment will be detailed in this paper. In the same manner as the wing, the boundary conditions for the pylon are applied at its mean camber plane. Similarly, the store boundary conditions are satisfied by a procedure identical to that used for the fuselage of the parent wing/fuselage arrangement.

Figure 2 depicts the crude-fine grid arrangement in the computational plane. The fine grid completely encloses the wing/pylon/store configuration and is embedded within a global crude grid. The fine grid involves a wing shearing transformation while the crude grid is in a Cartesian system.

Pylon Treatment

The pylon is a vertical wing-like surface whose mean camber plane is defined at a span station $y=y_p$. The boundary condition on either side of this surface is

$$[\phi_y(x,z)]_{y=y_p\pm}=[g'(x,z)]_{y=y_p\pm} \quad (2)$$

The presence of the pylon will require a special treatment for derivatives that are taken with respect to the spanwise direction y. After the shearing transformation that maps the wing into a rectangle, the derivatives that pass through the pylon are denoted as $\phi_{\eta\eta}$ and $\phi_{\xi\eta}$. Referring to Fig. 3, we illustrate the finite-differenced form for $\phi_{\eta\eta}$ and $\phi_{\xi\eta}$ at a grid

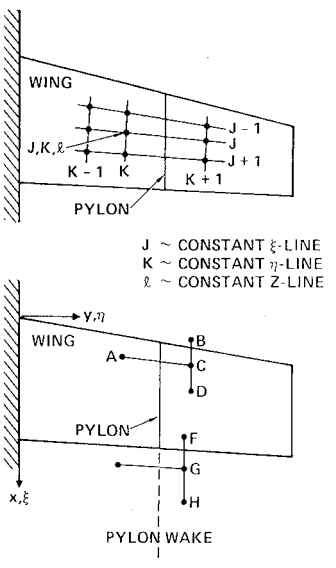

Fig. 3 Grid points neighboring pylon and pylon wake.

point (j,k,l) neighboring the pylon. (To demonstrate the ideas, a uniform mesh is assumed. In the actual code, the meshes are unequally spaced.) Thus,

$$(\phi_{\eta\eta})_{j,k,l} = (\phi_{j,k+1,l} - 2\phi_{j,k,l} + \phi_{j,k-1,l})/\Delta\eta^2$$

$$(\phi_{\eta\xi})_{j,k,l} = \frac{\phi_{j+1,k+1,l} - \phi_{j+1,k-1,l} - \phi_{j-1,k+1,l} + \phi_{j-1,k-1,l}}{4\Delta\eta\Delta\xi} \tag{3}$$

In both of the above expressions, $\phi_{j,k+1,l}$, $\phi_{j+1,k+1,l}$, and $\phi_{j-1,k+1,l}$ can be used only if they are not directly behind the pylon or the pylon wake. In Fig. 3, for example, the finite-differenced form of $\phi_{\eta\eta}$ and $\phi_{\xi\eta}$ at point A can make use of ϕ at point B but not the ϕ values at C and D because points C and D are behind the pylon while point B is not. Similarly, $\phi_{\eta\eta}$ and $\phi_{\xi\eta}$ at E cannot make use of ϕ at F, G, and H because F is behind the pylon and G and H are behind its wake. Thus, to finite difference the equation at points such as A or E, special procedures have to be developed to account for the pylon and pylon wake properly. These procedures are developed in much the same way the wing and wing wake are treated in the code, using image points.[3] If a constant ξ line cuts through the pylon, then image points are created on either side of the pylon as illustrated in Fig. 4. The values of the potential at these image points are obtained from the pylon slope information. For example, consider point A in Fig. 4. The image point in this case is point B. The potential value at this image point B can be obtained from the prescribed pylon slope information $g'(x,z)$ [Eq. (2)] at point C using the following central difference formula

$$(\phi_y)_{y_C} = [g'(x,z)]_{y_C} = (\phi_\eta + \phi_\xi \xi_y)_{y_C}$$

$$= \frac{\phi_B - \phi_A}{\Delta\eta} + (\phi_\xi \xi_y)_{y_C} \tag{4}$$

The image point information ϕ_B from Eq. (4) is then used in the finite-differenced form of $\phi_{\eta\eta}$ and $\phi_{\eta\xi}$ at point A. A similar procedure is used to evaluate the image point D that corresponds to the field point F, from the slope information $g'(x,z)$ at point E.

$$(\phi_y)_{y_E} = [g'(x,z)]_{y_E} = (\phi_\eta + \phi_\xi \xi_y)_{y_E}$$

$$= \frac{\phi_F - \phi_D}{\Delta\eta} + (\phi_\xi \xi_y)_{y_E} \tag{5}$$

When a constant ξ line cuts through the pylon wake, a potential jump across this surface is imposed just as in the case of the wing wake.

The same pylon treatment applies to a tip-mounted winglet system as a special case.

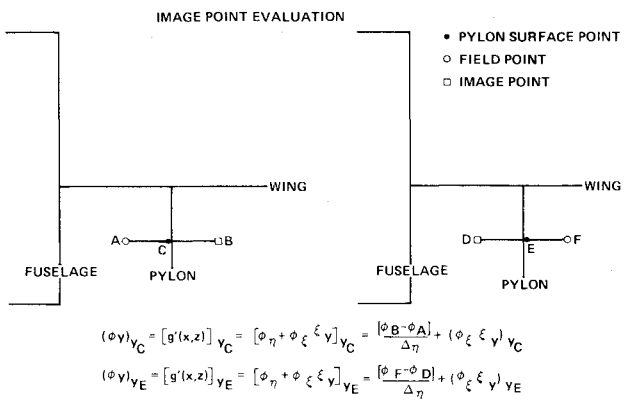

Fig. 4 Image point evaluation for pylon.

Store Treatment

For computational feasibility, the actual store is replaced by a prismatic surface as shown in Figs. 2 and 5. Slender body theory has been used to determine the appropriate modifications to the actual boundary conditions required when they are transferred to the computational prismatic support surface. Once the store shape is given, the Neumann boundary condition in terms of ϕ_z is known on the upper and lower store prismatic surfaces and in terms of ϕ_y on the two side surfaces. These boundary conditions are again implementable using the image point concept employed in the pylon analysis. For example, consider point D in Fig. 5 neighboring the store side surface. The finite-difference approximation for $\phi_{\eta\eta}$ and $\phi_{\xi\eta}$ at point D would require an estimate for the velocity potential at the image point E which can be obtained by central differencing the known Neumann data ϕ_y at point F as

$$(\phi_y)_{y_F} = (\phi_\eta + \phi_\xi \xi_y)_{y_F} = \frac{\phi_D - \phi_E}{\Delta\eta} + (\phi_\xi \xi_y)_{y_F} \tag{6}$$

The image point potential value ϕ_E is the only unknown in Eq. (6). Similarly, the image point B associated with point A neighboring the bottom store surface is obtained from

$$\phi_B = \phi_A + (z_B - z_A)(\phi_z)_C \tag{7}$$

The dummy point concept for the pylon and store described in Eqs. (4-7) greatly reduces the additional computer memory storage requirement and programming logic to include the pylon/store into a basic wing/fuselage code. This saving is particularly significant since the original wing/fuselage code itself practically saturates the entire CDC 7600 large and small core availability.

Computational Results

All of the calculations reported here were performed using the LBL CDC 7600 computer. A typical run involved 100 iterations on an initial grid $(40\times20\times20)$ followed by 100 iterations on a fine $(60\times30\times20)$-crude $(30\times20\times20)$ grid system. In addition to the foregoing memory savings, the complete wing/fuselage/pylon/store configuration calculations required practically the same amount of execution time as the clean arrangement. No computational penalty was paid with the image point concept employed to treat the pylon/store.

In general, attaching a pylon and store under a wing has considerable effect on the flowfield due to blockage of the side flow. Moreover, the associated redirection of the flow can result in acceleration to supercriticality in regions surrounding the store that were subsonic for the parent arrangement. Shocks can terminate these regions as in simpler flows.

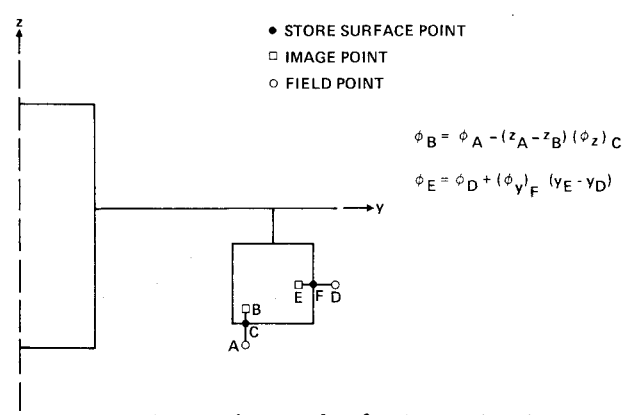

Fig. 5 Image point procedure for store treatment.

Experimental Comparisons

Figure 6 shows a slightly modified F-5 wing equipped with a pylon and store which was tested by Tijdemann and his coworkers.[4] The wing has, in part, modified NACA 65-A-004.8 sections, characterized by a droop nose, which extend from the leading edge toward the point of maximum thickness at 40% chord. Further aft, the profiles are symmetrical. Wind-tunnel results for this F-5 wing/pylon/store model are presented in Ref. 4. The same geometry, except the fins on the store, was used in the computational treatment. In the example, the leading edge of the pylon is swept forward. However, the pylon treatment reported in this paper is general enough to accommodate sweptback or sweptforward pylons. Although no instabilities were encountered for the pylon sweep angles discussed herein, values of sweep angles of the order of 50 deg or more could cause convergence problems similar to those associated with large wing sweep. Figure 6 also shows the comparison of computational and experimental span load distributions at $M_\infty = 0.9$ and $\alpha_W = \alpha_S = 0.5$ deg, where α_S and α_W are the store and wing angles of attack, respectively. The results indicate that the store/pylon creates a decrease of the loading which is maximum just inboard of the pylon. A discontinuity in this distribution at the pylon span location is also evident. This jump is associated with the pressure jump across the pylon at its line of attachment with the lower side of the wing and a continuous pressure across the same line on the upper wing surface. Discontinuities of the type described here are evident in the lower speed studies of Mangler[6] and Weber.[7,8]

Figure 7 shows a comparison of detailed chordwise pressure distributions between the computational and experimental results for the clean wing and the wing with the pylon/store at the span station neighboring the pylon for the configuration shown in Fig. 6. The appreciable suction peak at the leading edge of the lower surface is due to the droop nose of the wing airfoil.

Parametric Studies

On the basis of the earlier remarks concerning store integration, parametric studies have been performed to explore potential L/D benefits associated with optimum store arrangements. It will be seen that a proper choice for the pylon shape, store length, diameter, and its axial position can produce a higher L/D than that of the parent wing/fuselage configuration, due to beneficial nonlinear, nonplanar interference. Having established some validation of the computational model with experiments for the F-5 wing/pylon/store, we will apply the computational model of this paper to study the role of the aforementioned parameters as well as angle of attack and Mach number on aerodynamic quantities such as L/D, C_m, etc. For this study, the parent wing/fuselage configuration used by Alford et al.[5] has been chosen. The pylon used in all the parametric studies to be reported here is a rectangular planform flat plate extending from the leading edge of the wing to the trailing edge with a vertical height denoted by h in Fig. 1. The store radius distribution is given by $R(x)$ and its length by l. For all the calculations discussed here the store length l has been arbitrarily chosen to be 1.5 times the mean chord of the wing. The computational store treatment which utilizes an infinite-store support surface is expected to yield good results only when the store length is sufficiently large compared to the wing mean chord. Because of the confluence of singularities associated with stagnation point flows, a store whose nose and base are situated in the vicinity of the wing leading and trailing edges, respectively, will lead to convergence problems. Furthermore, the slender body boundary condition applied herein for the store is only valid away from the ends of the store where stagnation singularities occur, even in the isolated store case. For the examples treated here, the assumed store with length of 1.5 times the mean chord did not pose any convergence problem.

Figure 8 shows the effect of the pylon/store spanwise mounting location on the spanwise loading at Mach number 0.8 and wing angle of attack α_W, store angle of attack α_S, and fuselage angle of attack α_F, all kept at 5.8 deg. In this plot, the pylon height is kept fixed at -7 length units and the store diameter is 7.94 units, while the semispan b is 30 units. From the results, the previously observed discontinuity in connection with the F-5 configuration is also evident for this arrangement. As the pylon/store is moved toward the wing tip, the magnitude of this jump increases. Presumably, this is due to the pylon/store encountering a larger side wash toward the tip, causing greater side loads on the pylon. Figure 8 also shows the spanwise lift distribution for the wing/fuselage alone. For this configuration, the overall lift increases with the addition of the pylon/store with, however, a corresponding augmentation in drag, resulting in a net L/D penalty as compared to the parent configuration. In general, the degree of L/D alteration can be optimized by proper orientation of the pylon/store. As a first illustration, Fig. 9 indicates the effect of pylon height h and pylon span mounting location y_p on inviscid aerodynamic efficiency. Results from three different pylon heights and three different span mounting locations are shown. The quantity $[\Delta(L/D)/(L/D)_{W+F}]$ refers to the relative change in L/D due to pylon/store addition. Here $\Delta(L/D)$ is defined as

$$\Delta(L/D) = (L/D)_{W+F+P+S} - (L/D)_{W+F} \tag{8}$$

In Eq. (8) subscripts $W,F,P,$ and S refer to the wing, fuselage, pylon, and store, respectively. Figure 9 clearly indicates that the loss in L/D is minimized when the pylon/store is mounted around 50% span where the combination of tip effects and fuselage effects are probably minimal. For example, for

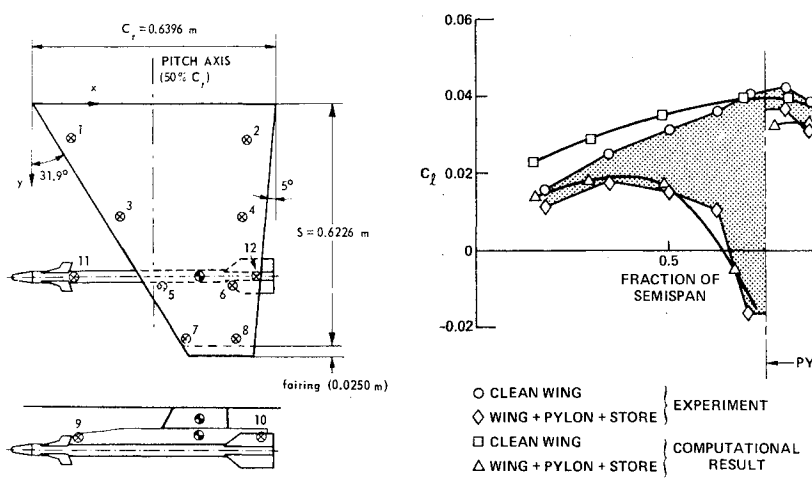

Fig. 6 Comparison of experimental and computational spanwise normal load distributions on the clean wing and on the wing with pylon and store ($M_\infty = 0.9$, $\alpha_W = \alpha_S = 0.5$ deg).

$h/b = 0.234$ and at 50% span mounting location gives a 4% penalty in L/D or range at fixed Mach number, specific fuel consumption, and weight ratio according to the Breguet range equation.

Figure 10 shows the effect of pylon height and pylon span location on pitching moment coefficient C_m. An increase in the moment coefficient due to the store addition will result in a higher trim drag. The computational model described herein is capable of providing optimum arrangements with a trim drag constraint as well as others such as landing clearance heights. As an indication of trim drag impact, Fig. 10 indicates that the quantity $\Delta C_m/(C_m)_{W+F}$ representing the relative changes in C_m and trim drag is smaller when the pylon/store is in the range 45-60% of span for this research configuration. Similar evaluations are feasible for more practical shapes.

The effect of other parameters on L/D are explored in Fig. 11. Influence of store diameter and span mounting location are shown at $M_\infty = 0.8$ and $\alpha_W = \alpha_S = \alpha_F = 3.8$ deg. Here again, the L/D penalty appears minimal when the store/pylon is around the 50% span location.

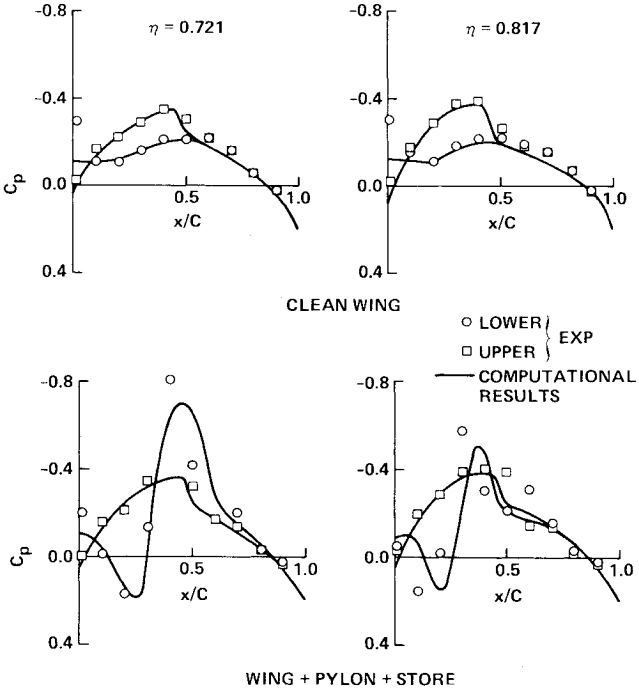

Fig. 7 Comparison of experimental and computational chordwise pressure distributions on F-5 wing with and without store/pylon ($M_\infty = 0.9$, $\alpha_W = \alpha_S = 0.5$ deg).

Based on Figs. 9-11 it is evident that for this configuration and flight conditions, a nearly 50% span mounting position gives the smallest penalty in aerodynamic efficiency.

The off-design performance of an optimum store/pylon location over a nonoptimum location is shown in the next four figures. For this study, a nearly 50% span mounting location is considered optimum and a 30% span location is considered nonoptimum. Figure 12 shows the effect of angle of attack on the $[\Delta(L/D)/(L/D)_{W+F}]$ performance. The □ symbol is for a 50% span position and the △ symbol corresponds to a 30% location. Clearly indicated is the fact that the off-design performance for the 50% span mounted pylon/store is superior to that for the 30% arrangement. Figure 13 shows a similar off-design study with Mach number. Again, the 50% arrangement appears best. Results such as these and the foregoing can be used as a basis for selection of optimum mission flight conditions by the designer with considerable wind-tunnel cost reduction.

Thus far, we have discussed primarily a computational treatment for nonplanar interference. Purely computational solutions for nonlinear problems by virtue of their complicated logic are somewhat expensive for quick turnaround design studies and tend to provide limited insight into the underlying physical mechanisms. To augment such understanding and provide cost effective design information, analytical procedures are being developed. One of these procedures is discussed in the next section.

Immersion Concept for Transonic Store Loads

Here, emphasis is placed on loads from the standpoint of store separation from the parent vehicle. This viewpoint

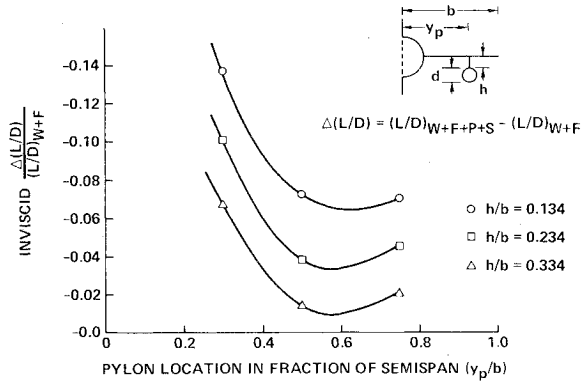

Fig. 9 Effect of pylon height h and pylon span mount location y_p on inviscid L/D performance ($M_\infty = 0.8$, $\alpha_F = \alpha_W = \alpha_S = 3.8$ deg).

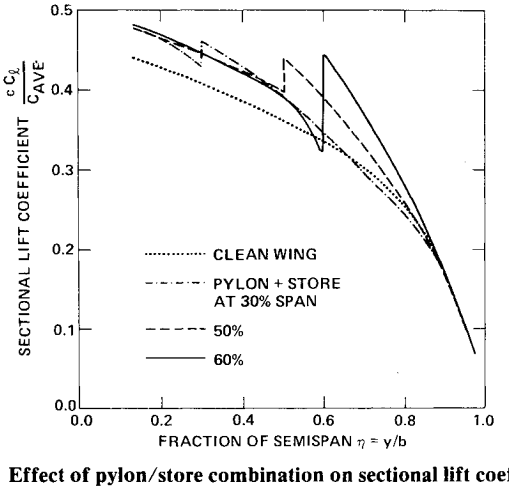

Fig. 8 Effect of pylon/store combination on sectional lift coefficient ($M_\infty = 0.8$, $\alpha_W = \alpha_F = \alpha_S = 5.8$ deg).

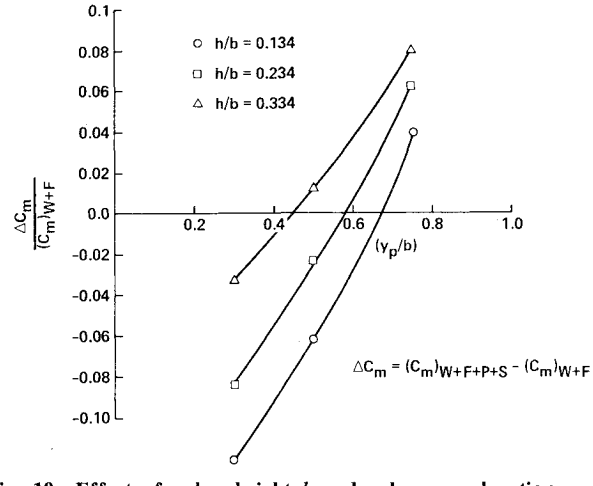

Fig. 10 Effect of pylon height h and pylon span location y_p on pitching moment coefficient C_m ($M_\infty = 0.8$, $\alpha_F = \alpha_W = \alpha_S = 3.8$ deg).

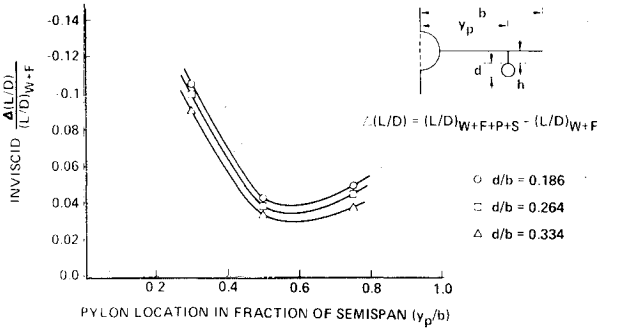

Fig. 11 Effect of store diameter d and pylon span mounting location y_p on inviscid L/D performance ($M_\infty = 0.8$, $\alpha_F = \alpha_W = \alpha_S = 3.8$ deg).

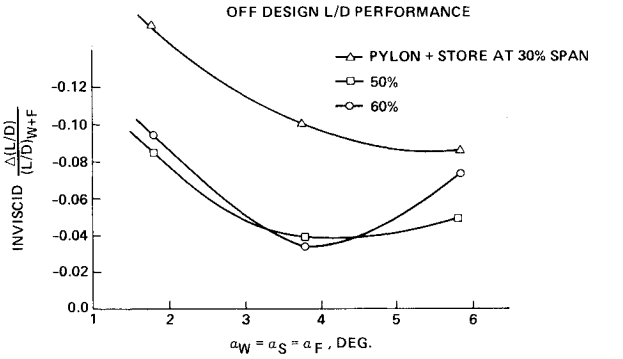

Fig. 12 Effect of angle of attack and pylon span location on inviscid L/D performance ($M_\infty = 0.8$).

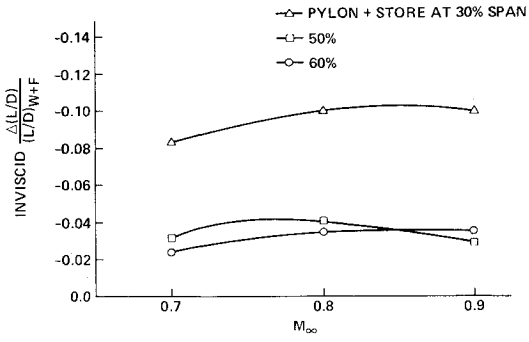

Fig. 13 Effect of Mach number on inviscid L/D performance ($\alpha_W = \alpha_S = \alpha_F = 3.8$ deg).

contrasts with the integration problem in which attention is given to the alterations of the vehicle loads due to the store. An immersion model has been used in a manner in which the effect on the store is assumed to be "one-way" in the sense that its incidence environment is due to the isolated parent vehicle, which for this nonlinear transonic case is computationally established. Feedbacks or two-way interactions involving the alteration of this field due to the presence of this store will be initially neglected.

Using classical slender body theory,[9] the normal force coefficient C_N for the store is written as

$$C_N = [2S_B\alpha_B + (C_N)_{W+T}]/S_B \tag{9}$$

where

$$(C_N)_{W+T} = S_W[(K_W + K_B)C_{N_\alpha}\alpha]_W + S_T[(K_W + K_B)C_{N_\alpha}\alpha]_T \tag{10}$$

Here subscripts W, T, and B refer to store wing, store tail, and store body, respectively. In Eqs. (9) and (10), S_B represents the base area and K_W and K_B represent interference factors associated with the interaction of the body with wing-like surfaces. These interaction factors are obtained from slender body theory.[9]

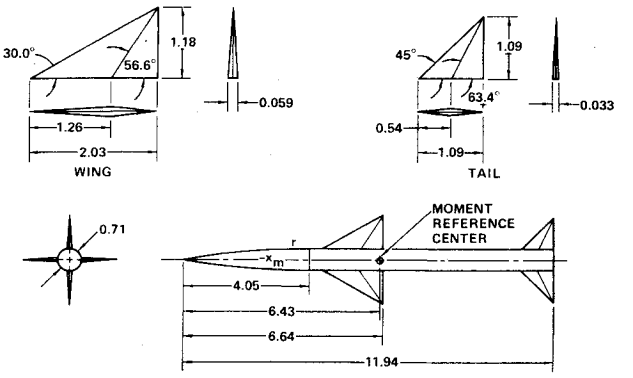

Fig. 14 Store model used in immersion theory calculations.

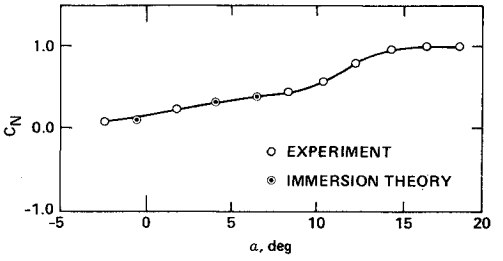

Fig. 15 Store aerodynamic forces in presence of wing/fuselage/pylon combination for various Mach numbers (comparison of immersion theory and experiments).

For the store geometry shown in Fig. 14, we obtain finally the following relation

$$C_N = (1/57.3)(0.3314\alpha_B + 3.64\alpha_W + 2.54\alpha_T) \tag{11}$$

where α is in degrees. An estimate for α_B, α_W, and α_T is obtained from the resultant flow angularity calculations for the parent wing/fuselage configuration using the transonic code. The angles α_B for the store body, α_W for the store wing, and α_T for the store tail used in Eq. (11) are average angles of attack over the lifting surfaces of these components. Application of Eq. (11) using the transonic code downwash fields yields the comparison with experimental results indicated in Fig. 15. In view of the number of assumptions made, the good agreement of the elementary model is surprising. The quality of this comparison suggests the utility of this approach when coupled with a computational model for the downwash on the parent configuration to obtain results for many store locations economically.

Conclusions

Computational and analytical results for transonic store/pylon configurations have been presented. The approach demonstrates:

1) The use of an image point concept in incorporating the pylon/store requires minimum additional memory, programming logic, and execution time.

2) Substantial aerodynamic efficiency enhancements are feasible in the transonic regime with proper pylon/store locations.

3) Computational models are "rich" enough to reproduce such experimentally observed features as span load discontinuities across the pylon and reflected shock patterns.

4) Immersion theory when combined with the nonlinear parent wing code can provide quick and reliable indications of

store loads and safe store launch locations in the transonic regime.

Acknowledgments

The effort described herein was supported by the Office of Naval Research under Contract N00014-78-C-0477, Project 212-257.

References

[1] Ballhaus, W.F., Bailey, F.R., and Frick, J., "Improved Computational Treatment of Transonic Flow About Swept Wings," *Advances in Engineering Sciences,* NASA CP-2001, 1976.

[2] Mason, W.H., MacKenzie, D.A., Stern, M.A., Ballhaus, W.F., and Frick, J., "An Automated Procedure for Computing the Three-Dimensional Transonic Flow Over Wing-Body Combinations, Including Viscous Effects," Air Force Flight Dynamics Laboratory, TR-77-122, Vol. I, Oct. 1977.

[3] Shankar, V., Malmuth, N.D., and Cole, J.D., "A Computational Transonic Inverse Procedure for Three-Dimensional Wings and Wing-Body Combinations," AIAA Paper No. 79-0344.

[4] Tidjemann, H., Nunen, J.W.G.V., Kraan, A.N., Persoon, A.J., Poestkokes, R., Roos, R., Schippers, P., and Siebert, C.M., "Transonic Wind-Tunnel Tests on an Oscillating Wing with External Store, Part IV: The Wing with Underwing Store," National Aerospace Laboratory, The Netherlands, Rept. NLR TR 78106 U, Part IV, 1979.

[5] Alford, W.J. and King, T.J., "Experimental Static and Aerodynamic Forces and Moments at High Subsonic Speeds on a Missile Model during Simulated Launching from a Semispan Location of a 45 deg Swept-Wing-Fuselage-Pylon Combination," NACA RML56J05, Jan. 10, 1957.

[6] Mangler, W., "Lift Distribution Around Airfoils with End-plates," L.F.F., Vol. 16, 1939, p. 219, ARC 8237, Dec. 1944 (RTP Trans. 2338).

[7] Weber, J., "Theoretical Load Distribution on a Wing with Vertical Plates," ARC Technical Rept. R&M 2960, 1956.

[8] Weber, J. and Lawford, J.A., "The Reflection Effect of Fences at Low Speeds," ARC 17060, May 1954.

[9] Pitts, W.C., Nielsen, J.N., and Kaatari, G.E., "Lift and Center of Pressure of Wing-Body-Tail Combinations at Subsonic, Transonic, and Supersonic Speeds," NACA Technical Rept. 1307, 1957.